

# A Mimimum Time Velocity scheduling method for single-axis movement

Shuyang Dai<sup>1</sup> and Feiyu Zhu<sup>2</sup>

<sup>1</sup>School of Mathematics and Statistics, Wuhan University

<sup>2</sup>Wuhan Britain China School

## Abstract

In this paper, we propose a velocity planning method based on a three-phase S-curve, which can achieve the shortest motion time given the initial and final positions as well as the initial and final velocities. The algorithm can achieve very high accuracy.

## 1 Introduction

The innovative spot-scanning proton arc (SPArc) therapy introduced by Ding et al.<sup>1</sup> generates a proton scanning plan consisting of hundreds of discrete irradiation angles. These angles, along with energy layers, spot placements, and monitor unit (MU) weightings, are optimized to ensure robustness. This method provides a more precise dose distribution to target volumes and achieves improved protection of organs-at-risk (OARs) compared to IMPT. In the process of proton beam delivering, it is important to design a continuous gantry rotation in order to improve the quality and robustness of the therapy.

However, abrupt shifts in acceleration, where the system switches instantaneously between its maximum value  $A_m$  and  $-A_m$  create a simple linear AD profile for gantry rotation. Such rapid changes can induce resonance effects, resulting in fatigue damage. To ensure smooth gantry velocity profiles and precise proton beam delivery, additional constraints on the gantry's kinematic properties are necessary.

Constraining the derivative of acceleration, also known as jerk (the time rate of change of acceleration), is a widely used technique to limit the variation of actuator torque. This approach is commonly applied in areas such as feedrate scheduling for computer numerically controlled (CNC) machining systems<sup>6–9</sup> and trajectory planning or optimization for industrial robotic manipulators<sup>10–12</sup>. By introducing such constraints, smoother motion and reduced machine wear can be achieved<sup>5</sup>.

Inspired by these practices, we introduce an innovative gantry motion scheduling method that generates a smooth velocity profile for gantry transitions between consecutive angles. This method enforces bounds on jerk, acceleration, and velocity, ensuring a time-optimal transition between velocity values under the given constraints. Furthermore, it accommodates the specified velocities at adjacent gantry positions to maintain precision.

## 2 S-shape velocity planning

The procedure for gantry movement planning from one angle to the adjacent angle is equivalent to provide an algorithm for single-axis minimum time velocity profile generation with variable starting velocity and ending velocity, the key step of the algorithm is to determine the maximum reachable velocity. If the maximum achievable speed during motion is higher, and the time taken to transition from the initial speed to the maximum speed, as well as from the maximum speed to the final speed, is shorter under constraints, then the fastest motion planning for a single-axis movement can be achieved.

Since the motion process specifies that the speeds at the start and end points along a single axis are  $v_s$  and  $v_e$ , respectively, and the distance between the start and end points is  $d = (\text{end coordinate} - \text{start coordinate}) > 0$  (i.e., considering the case where the end coordinate is greater than the start coordinate; if the end coordinate is less than the start coordinate, the initial and final velocity values and the distance value need to be negated), the motion process can be divided into three segments:

- An acceleration segment from  $v_1$  to  $v_m$ ,
- A constant velocity segment at  $v_m$ ,

- A deceleration segment from  $v_m$  to  $v_2$ .

Here,  $v_m$  is the maximum achievable speed during the motion. The acceleration and deceleration segments both adopt a three-period S-shape strategy to achieve the fastest motion planning for  $v_1 \rightarrow v_m$  and  $v_m \rightarrow v_2$ .

## 2.1 The basic profile

In this section, we introduce a basic acceleration/deceleration (ACC/DEC) profile to switch the velocity from  $v_s$  to  $v_e$ , in which constraints on maximum jerk and acceleration are considered. Without loss of generality, we first derive the profile for the acceleration procedure, i.e.,  $v_s < v_e$ .

Assume that both jerk and acceleration are zero at the start and end points, the profile consists of three periods, as illustrated in Figure 1a.

1. The acceleration increases from 0 to  $a_m$  over a duration of  $t_1$  with jerk  $j_m$ ;
2. The acceleration remains constant for a duration of  $t_2$ ;
3. The acceleration decreases from  $a_m$  to zero over a duration of  $t_1$ , with the velocity reaching its maximal value  $v_m$ .

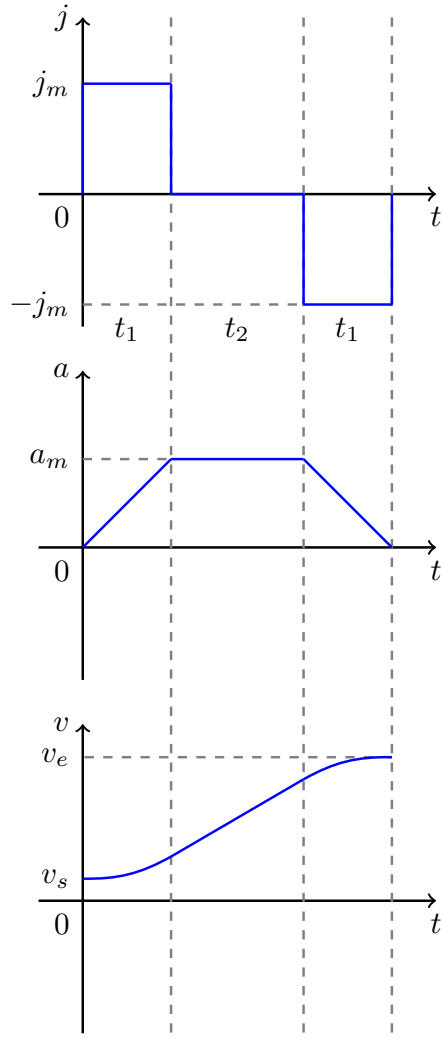
Analytical expressions for  $j(t)$ ,  $a(t)$  and  $v(t)$  are given by Equations (1a)-(1c).

$$j(t) = \begin{cases} j_m, & 0 \leq t < t_1, \\ 0, & t_1 \leq t < t_1 + t_2, \\ -j_m, & t_1 + t_2 \leq t < 2t_1 + t_2, \end{cases} \quad (1a)$$

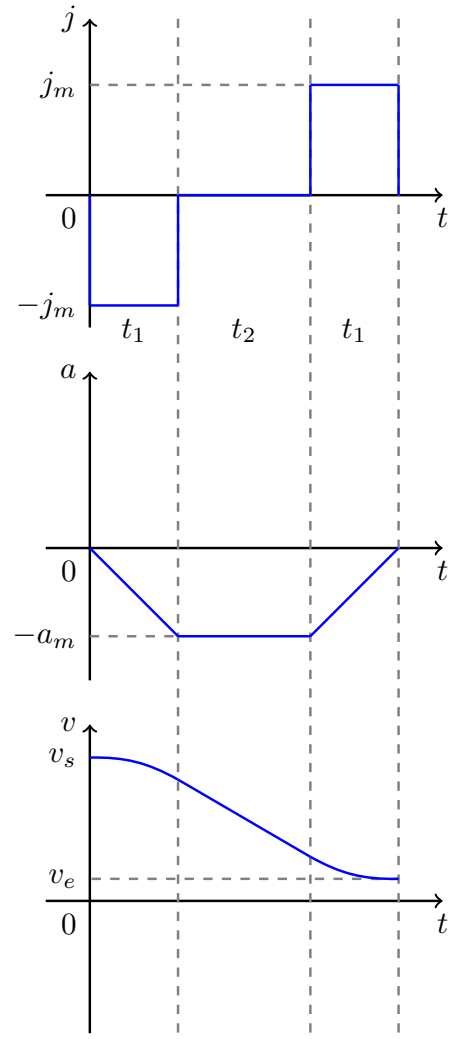
$$a(t) = \begin{cases} j_m t, & 0 \leq t < t_1, \\ j_m t_1, & t_1 \leq t < t_1 + t_2, \\ j_m(2t_1 + t_2 - t), & t_1 + t_2 \leq t < 2t_1 + t_2, \end{cases} \quad (1b)$$

$$v(t) = \begin{cases} v_s + \frac{1}{2}j_m t^2, & 0 \leq t < t_1, \\ v_s + j_m t_1 t - \frac{1}{2}j_m t_1^2, & t_1 \leq t < t_1 + t_2, \\ v_s - \frac{1}{2}j_m(2t_1 + t_2 - t)^2 \\ + j_m(t_1^2 + t_1 t_2), & t_1 + t_2 \leq t < 2t_1 + t_2. \end{cases} \quad (1c)$$

We observe that the maximal acceleration is reached at  $t = t_1$ , i.e.,  $a_m = j_m t_1$ , the velocity increment is expressed as  $\Delta v = a_m(t_1 + t_2)$ .



(a) ACC



(b) DEC

Figure 1: The three-period profile

The three-period profile yields a continuous acceleration function, a differentiable velocity function, and a  $C^2$  continuous distance function. If either jerk or acceleration (or both) can reach their boundary values, i.e.,  $j_m = \pm J_m$ ,  $a_m = \pm A_m$ , the profile exhibits bang-bang control<sup>4,15</sup>, implying that it is the time optimal procedure to switch from  $v_s$  to  $v_e$ . If  $v_s > v_e$ , the profile can be applied in reverse for deceleration, as shown in Figure 1b.

Set  $j_m = J_m$  and  $a_m = A_m$ , then  $t_1$  and  $t_2$  can be determined by

$$t_1 = \frac{A_m}{J_m}, \quad t_2 = \frac{v_e - v_s}{A_m} - \frac{A_m}{J_m}. \quad (2)$$

Since  $t_2$  is required to be no less than zero, i.e.,  $v_e - v_s \geq A_m^2/J_m$ ,  $a(t)$  exhibits trapezoidal shape. If the required velocity increment  $v_e - v_s$  does not satisfy this condition, then  $A_m$  can not be reached, otherwise the resulting velocity through the trapezoidal profile starting from  $v_s$  will exceed  $v_e$ . Therefore,  $t_2$  must be zero when  $v_e - v_s < A_m^2/J_m$ , and  $a(t)$  exhibits triangular shape. The complete expressions for  $t_1$  and  $t_2$  are given by Equation (3).

$$\begin{cases} t_1 = \frac{A_m}{J_m}, \quad t_2 = \frac{v_e - v_s}{A_m} - \frac{A_m}{J_m}, & \text{if } v_e - v_s \geq \frac{A_m^2}{J_m}, \\ t_1 = \sqrt{\frac{v_e - v_s}{J_m}}, \quad t_2 = 0, & \text{if } v_e - v_s < \frac{A_m^2}{J_m}. \end{cases} \quad (3)$$

For the deceleration case,  $t_1$  and  $t_2$  can be determined by substituting  $v_s - v_e$  for  $v_e - v_s$  in Equation (3).

The total duration and distance are determined by

$$t = 2t_1 + t_2, \quad d = \frac{1}{2} (v_s + v_e) (2t_1 + t_2). \quad (4)$$

## 2.2 The jerk-limited ACC/DEC profile with distance constraint

In this section, we present the jerk-limited ACC/DEC profile to switch the velocity from  $v_s$  to  $v_e$  within a specified distance  $d_m$ . Without loss of generality, we assume that  $v_s < v_e$ .  $d_m$  is given as a linear function of  $v_s$  and  $v_e$ , i.e.,

$$d_m = d - \frac{1}{2} (v_s t_s + v_e t_e), \quad (5)$$

where  $d, t_s$  and  $t_e$  are constants. Let  $V_m$  denote the maximum velocity.

The profile consists of three phases: first, increase the velocity from  $v_s$  to  $V_m$ ; second, maintain the velocity at  $V_m$  for a while; third, decrease the velocity from  $V_m$  to  $v_e$ . In the acceleration and deceleration phases, the three-period profile with  $J_m$  and  $A_m$  introduced in Section 2.1 is utilized. The time parameters for the acceleration phase are denoted by  $t_1, t_2$ , while  $t_3$  represents the duration of the constant velocity phase, and  $t_4, t_5$  correspond to the deceleration phase.

Let  $d_i$  and  $d_d$  represent the distances required to increase from  $v_s$  to  $V_m$ , and to decrease from  $V_m$  to  $v_e$ .  $d_i$  and  $d_d$  can be computed by substituting the pairs  $(v_s, V_m)$  and  $(v_e, V_m)$  into Equations (3) and (4). However, if  $d_m$  is not long enough, the velocity can not reach  $V_m$  from  $v_s$ ; or  $d_m$  is so short that the velocity can not even reach  $v_e$  from  $v_s$ , where  $v_e$  needs to be adjusted. Therefore, three cases remain to be discussed.

**Case 1.** If  $d_m \geq d_i + d_d$ , then the velocity can reach  $V_m$  within  $d_m$ , and the duration of the constant velocity phase is given by  $t_3 = (d_m - d_i - d_d) / V_m$ .

**Case 2.** If  $d_m < d_i + d_d$ , then the velocity can not reach  $V_m$  within  $d_m$ , resulting in  $t_3 = 0$ . Let  $t_1, t_2$  denote the time parameters for the three-period profile to increase from  $v_s$  to  $v_e$ , compute  $d_0$  by

$$d_0 = \frac{1}{2} (v_s + v_e) (2t_1 + t_2). \quad (6)$$

If  $d_m \geq d_0$ , a reachable maximal velocity  $v_m \in [v_e, V_m)$  exists for the velocity to first increase from  $v_s$  to  $v_m$  and then decrease from  $v_m$  to  $v_e$ . Let  $\hat{t}_1, \hat{t}_2$  denote the time parameters for the acceleration phase and  $\hat{t}_4, \hat{t}_5$  for the deceleration phase, then  $v_m$  must satisfy the following condition:

$$d_m = \frac{1}{2} (v_s + v_m) \hat{t}_{m1} + \frac{1}{2} (v_s + v_m) \hat{t}_{m2}, \quad (7)$$

where  $\hat{t}_{m1} = 2\hat{t}_1 + \hat{t}_2$  and  $\hat{t}_{m2} = 2\hat{t}_4 + \hat{t}_5$ . Note that the function on the right-hand side is monotonic with respect to  $v_m \in [v_e, V_m]$  ensuring the existence of a unique root in  $[v_e, V_m]$  for Equation (7). We employ a bisection method<sup>4</sup> to solve for  $v_m$ .

**Case 3.** If  $d_m < d_0$ , then the velocity can not reach  $v_e$  within  $d_m$ , leading to  $t_3 = t_4 = t_5 = 0$ . However, there exists a reachable end velocity  $\hat{v}_e \in [v_s, v_e)$ . Let

$\hat{t}_1, \hat{t}_2$  be the time parameters to increase from  $v_s$  to  $\hat{v}_e$ , then  $\hat{v}_e$  must satisfy the following condition:

$$d = \frac{1}{2} (v_s t_s + \hat{v}_e t_e) + \frac{1}{2} (v_s + \hat{v}_e) \hat{t}_m, \quad (8)$$

where  $\hat{t}_m = 2\hat{t}_1 + \hat{t}_2$ . Similarly,  $\hat{v}_e$  is solved from Equation (8) using the bisection method.

### 3 Results

We will utilize the motion planning for single-axis movement based on the following examples.

- **Case 1**

The constrain is  $J_m = 2 \times 10^3, A_m = 20, V_m = 1.2$ :

Table 1: Parameters for Case 1

	Start Position	End Position	Initial Velocity	End Velocity
Case: Ex1	0.000	0.033	0.00	0.00
Case: Ex2	0.000	0.033	0.00	0.03
Case: Ex3	0.000	0.000	0.00	0.40
Case: Ex4	0.000	0.033	0.00	1.20

- **Case 2**

The constrain is  $J_m = 1.2 \times 10^4, A_m = 40, V_m = 0.8$ :

The specific computational results for the corresponding maximum speeds and result errors presented in Table 3. In each set of examples. From the results, it can be observed that the algorithm achieves very high accuracy in the single-axis motion planning part under continuous conditions.

Table 2: Parameters for Case 2

	Start Position	End Position	Initial Velocity	End Velocity
Case: Ex5	0.000	0.033	0.00	0.00
Case: Ex6	0.000	0.033	0.00	0.03
Case: Ex7	0.000	0.000	0.00	0.40
Case: Ex8	0.000	0.033	0.00	1.20

Table 3: Maximum speeds and resultant errors

Case 1	Ex1	Ex2	Ex3	Ex4
$v_m$	0.6367	0.6333	-0.2425	-0.3821
End Position Error	2.0817e-17	6.9388e-18	5.9496e-18	1.3878e-17
Final Velocity Error	0.0000e0	1.3878e-16	0.0000e0	0.0000e0
Case 2	Ex5	Ex6	Ex7	Ex8
$v_m$	0.6832	0.6766	-0.2338	-0.1915
End Position Error	6.9389e-18	6.9389e-18	5.2855e-19	0.0000e0
Final Velocity Error	5.5511e-17	2.3592e-16	0.0000e-0	2.2204e-16

## References

- [1] Xuanfeng Ding, Xiaoqiang Li, J. Michele Zhang, Peyman Kabolizadeh, Craig Stevens, and Di Yan. Spot-Scanning Proton Arc (SPArc) Therapy: The First Robust and Delivery-Efficient Spot-Scanning Proton Arc Therapy. *International Journal of Radiation Oncology\*Biology\*Physics*, 96(5):1107–1116, December 2016.
- [2] Xiaoqiang Li, Gang Liu, Guillaume Janssens, Olivier De Wilde, Vincent Bossier, Xavier Lerot, Antoine Pouppez, Di Yan, Craig Stevens, Peyman Kabolizadeh, and Xuanfeng Ding. The first prototype of spot-scanning proton arc treatment delivery. *Radiotherapy and Oncology*, 137:130–136, August 2019.



- [3] Gang Liu, Lewei Zhao, Peilin Liu, Di Yan, Rohan Deraniyagala, Craig Stevens, Xiaoqiang Li, and Xuanfeng Ding. Development of a standalone delivery sequence model for proton arc therapy. *Medical Physics*, page mp.16879, December 2023.
- [4] Wei Fan, Xiao-Shan Gao, Wei Yan, and Chun-Ming Yuan. Interpolation of parametric CNC machining path under confined jounce. *The International Journal of Advanced Manufacturing Technology*, 62(5-8):719–739, September 2012.
- [5] Hasti Hayati, David Eager, Ann-Marie Pendrill, and Hans Alberg. Jerk within the Context of Science and Engineering—A Systematic Review. *Vibration*, 3(4):371–409, October 2020.
- [6] Kaan Erkorkmaz and Yusuf Altintas. High speed CNC system design. Part I: jerk limited trajectory generation and quintic spline interpolation. *International Journal of Machine Tools and Manufacture*, 41(9):1323–1345, July 2001.
- [7] Jingyan Dong, P.M. Ferreira, and J.A. Stori. Feed-rate optimization with jerk constraints for generating minimum-time trajectories. *International Journal of Machine Tools and Manufacture*, 47(12-13):1941–1955, October 2007.
- [8] YuWen Sun, ManSen Chen, JinJie Jia, Yuan-Shin Lee, and DongMing Guo. Jerk-limited feedrate scheduling and optimization for five-axis machining using new piecewise linear programming approach. *Science China Technological Sciences*, 62(7):1067–1081, July 2019.
- [9] Juliang Xiao, Sijiang Liu, Haitao Liu, Mingli Wang, Guangxi Li, and Yunpeng Wang. A jerk-limited heuristic feedrate scheduling method based on particle swarm optimization for a 5-DOF hybrid robot. *Robotics and Computer-Integrated Manufacturing*, 78:102396, December 2022.
- [10] S. Macfarlane and E.A. Croft. Jerk-bounded manipulator trajectory planning: design for real-time applications. *IEEE Transactions on Robotics and Automation*, 19(1):42–52, February 2003.

- [11] Jan Mattmüller and Damian Gisler. Calculating a near time-optimal jerk-constrained trajectory along a specified smooth path. *The International Journal of Advanced Manufacturing Technology*, 45(9-10):1007–1016, December 2009.
- [12] Yi Fang, Jin Qi, Jie Hu, Weiming Wang, and Yinghong Peng. An approach for jerk-continuous trajectory generation of robotic manipulators with kinematical constraints. *Mechanism and Machine Theory*, 153:103957, November 2020.
- [13] Viktor Wase, Otte Marthin, Albin Fredriksson, and Anton Finnson. Optimizing the traversal time for gantry trajectories for proton arc therapy treatment plans. *Physics in Medicine & Biology*, February 2024.
- [14] Gang Liu, Lewei Zhao, Peilin Liu, Riao Dao, Yujia Qian, Xiaoda Cong, Guillaume Janssens, Xiaoqiang Li, and Xuanfeng Ding. The first investigation of spot-scanning proton arc (SPArc) delivery time and accuracy with different delivery tolerance window settings. *Physics in Medicine & Biology*, 68(21):215003, November 2023.
- [15] Yifei Hu, Xin Jiang, Guanying Huo, Cheng Su, Shiwei Zhou, Bolun Wang, Hexiong Li, and Zhiming Zheng. A novel feed rate scheduling method with acc-jerk-continuity and round-off error elimination for non-uniform rational B-spline interpolation. *Journal of Computational Design and Engineering*, 10(1):294–317, January 2023.